Modern Research and Educational Topics in Microscopy.
A. Méndez-Vilas and J. Díaz (Eds.)

Single-Molecule Fluorescence Imaging Techniques for the Detection of Reactive Oxygen Species

T. Tachikawa and **T. Majima**

The Institute of Scientific and Industrial Research (SANKEN), Osaka University, Mihogaoka 8-1, Ibaraki, Osaka 567-0047, Japan

In this short account, we have focused on the methodology for the single-molecule detection of reactive oxygen species (ROS), such as hydroxyl radical ($HO^{\bullet}$) and singlet oxygen ($^1O_2$), using a total internal reflection fluorescence microscopy (TIRFM). A successful application using the single-molecule fluorescence techniques for the investigation of the TiO_2 photocatalytic oxidation reactions is briefly demonstrated.

Keywords single-molecule fluorescence spectroscopy; reactive oxygen species; TiO_2 photocatalyst

1. Introduction

Probing conformational dynamics, local environments, chemical interactions and reactions at the single-molecule level represents the ultimate degree of sensitivity for sensing and imaging [1-9]. For example, Adams et al. used single-molecule fluorescence techniques to follow electron transfer processes in donor-bridge-acceptor and molecular sensors systems [5]. They successfully detected various target species, such as H^+, Zn^+, Au, TiO_2, glass, and so on, at the single-molecule level. Recently, Hofkens and co-workers studied the spatial distribution of catalytic activity on a layered double hydroxide (LDH) consisting of prismatic crystals with large basal planes and lateral faces the entire crystal by using a wide field microscope [6]. The obtained fluorescence intensity distribution clearly indicates that the hydrolysis activity follows the contours of the crystal. From experimental results, they concluded that ester hydrolysis proceeds on the lateral {1010} crystal faces, while transesterification occurs on the entire outer crystal surface. More recently, Bräuchle and co-workers investigated the heterogeneity and the mechanistic details of diffusion processes of individual dye molecules inside mesoporous silica thin films using various single-molecule fluorescence techniques [8,9]. Indeed, the single-molecule spectroscopy can be applicable for various heterogeneous reaction systems.

The TiO_2 photocatalysts have been extensively studied and used for the water-splitting reaction that produces hydrogen, the degradation of organic pollutants, the surface wettability conversion, and so on [10-20]. It has been reported that various reactive oxygen species (ROS), such as superoxide radical ($O_2^{\bullet-}$), singlet oxygen ($^1O_2$), hydroxyl radical ($HO^{\bullet}$), and H_2O_2, are generated on the TiO_2 surface in the gas and liquid phases. Recently, Tatsuma et al. reported the remote photocatalytic oxidation of organic and inorganic materials using the TiO_2 photocatalyst [19,20]. They explained this phenomenon in terms of a double excitation scheme in which the photodecomposition of gaseous H_2O_2 by UV light to give $HO^{\bullet}$ is the key process.

The scientific research in the field of ROS associated with biological and non-biological functions is continuously requiring new sensitive and specific tools that may enable a deeper insight on its action mechanisms. However, ROS present some characteristics that make them difficult to be detected, namely their very short lifetime and high reactivity, and the variety of antioxidants existing in vivo, capable of capturing these species. It is, therefore, essential to develop methodologies capable of overcoming this type of obstacles. The fluorescence methodology, associated with the use of suitable probes, is an excellent approach to measure ROS because of its high sensitivity, simplicity in data collection, and high spatial resolution in microscopic imaging techniques [21. In particular, the metastable and reactive ROS, such as $^1O_2$ and $HO^{\bullet}$, have a finite lifetime in any system in which it is produced. The magnitude of this

lifetime can vary over a large range and is governed by the constituents of the medium in which ROS exist. Thus, much would be gained if tenuous ROS in air, solution, polymer, and biological systems could be directly monitored with both time and spatial resolutions.

The main goal of this short account is to present the fluorescence methodologies that have been used for detecting ROS, especially, $^1O_2$, at the single-molecule level. First, we introduce the experimental procedures to detect ROS generated during TiO_2 photocatalytic reactions using TIRFM [22]. Next, we introduce our recent works for the detection of airborne ROS. The authors and co-workers have successfully applied the single-molecule techniques to clarify the bleaching processes of single dye molecules during the remote TiO_2 photocatalytic oxidation reactions. Moreover, an airborne $^1O_2$ molecule diffused from the surface of the TiO_2 nanoparticles was detected at the single-molecule level [23]. Finally, we summarize our contributions with some future directions for the applications of the single-molecule spectroscopy toward the heterogeneous reaction systems.

2. Experimental

2.1 Total internal reflection fluorescence microscopy (TIRFM)

TIRFM can be used to observe fluorophores attached onto a glass surface, biomolecules, and living cells [24-27]. The illumination method utilized for the excitation of fluorophores in TIRFM is conceptually simple. When the excitation light for fluorophores is incident above some critical angle upon the glass/liquid interface, the light is totally internally reflected and generates a thin electromagnetic field, so-called "evanescent field", in a medium with the same wavelength as the incident light. When the electromagnetic wave is permitted to penetrate into only a limited depth as explained by Maxwell's equations, the intensity of the transmitted wave, $\boldsymbol{I}_T$, is given by

$$\boldsymbol{I}_T = \left|\boldsymbol{A}_T\right|^2 \exp\left[-z\frac{4\pi}{\lambda_2}\sqrt{\frac{\sin^2\theta}{n^2}-1}\right], \tag{1}$$

where $\boldsymbol{A}_T$, z, λ_2, and θ are the amplitude of the electric field, the wavelength in medium 2, the perpendicular distance from the interface, and the angular frequency in medium 2, and the incidence angle, respectively, and $n = n_2/n_1$ (= $\sin\theta_c$), where n_1, n_2, and θ_c are refractive indices for media 1 and 2, and the critical angle, respectively. The intensity of the evanescent field decays exponentially with the distance from the glass surface. The penetration depth d, i.e., 1/e value in Equation (1), is also given by

$$d = \frac{\lambda}{4\pi\sqrt{n_1^2\sin^2\theta - n_2^2}}, \tag{2}$$

where λ (= $n_2\lambda_2$) is the wavelength of the incident light in vacuum.

To date, two different technical solutions for TIR illumination, i.e., prism-type and objective-type TIRM, have been established. Here, we will describe the optical configuration of objective-type TIRFM based on an inverted microscope as illustrated in Figure 1. A high numerical aperture objective lens is mounted on an inverted microscope. A laser beam passed through a neutral density filter (ND) is focused by a lens on the back focal plane of the objective. By shifting the laser position, the path of the incident laser light is shifted from the center to the edge of the objective. At the center position, the microscope can be used as a standard epi-fluorescence microscope.

In our experimental setup, light emitted from a continuous wave (CW) Nd:YAG laser (532 nm, 50 mW; JDS Uniphase) or a CW Ar ion laser (488 nm, 10 mW; Melles Griot) passing through an objective lens (Olympus, PlanApo, 1.40 NA, 100×) was totally reflected at the coverslip-air interface to obtain an evanescent field which can excite a dye molecule.

For imaging, the fluorescence emission from single dyes was collected using an oil-immersion microscope objective and intensified by an image intensifier (Hamamatsu Photonics, C8600-03) coupled

to a CCD camera (Hamamatsu Photonics, C3077-70). The images were recorded on a video cassette recorder at the video frame rate of 30 frames s^{-1} for further analysis. The pictures recorded on the videotape were converted into an electronic movie file using the ADVC 1394 video capture board (Canopus). Changes in the fluorescence intensity of the spots were analyzed using the mean gray scale in the region of interest, which was performed using Scion Image software (http://www.scioncorp.com).

For spectroscopy, only the fluorescence that passed through a slit was brought into an imaging spectrograph (Acton Research, SP-2356) equipped with an electron-multiplying charge coupled device (EM-CCD) camera (Princeton Instruments, PhotonMAX:512B). The width of the slit was 50 μm, which corresponded to 0.5 μm at the specimen, because the images at the slit were magnified by 100×. The spectra were typically integrated for 10 s. The fluorescence spectra were cut by a dichroic mirror and a long-pass filter on the blue edge. The spectrum detected by the EM-CCD camera was stored and analyzed by a personal computer.

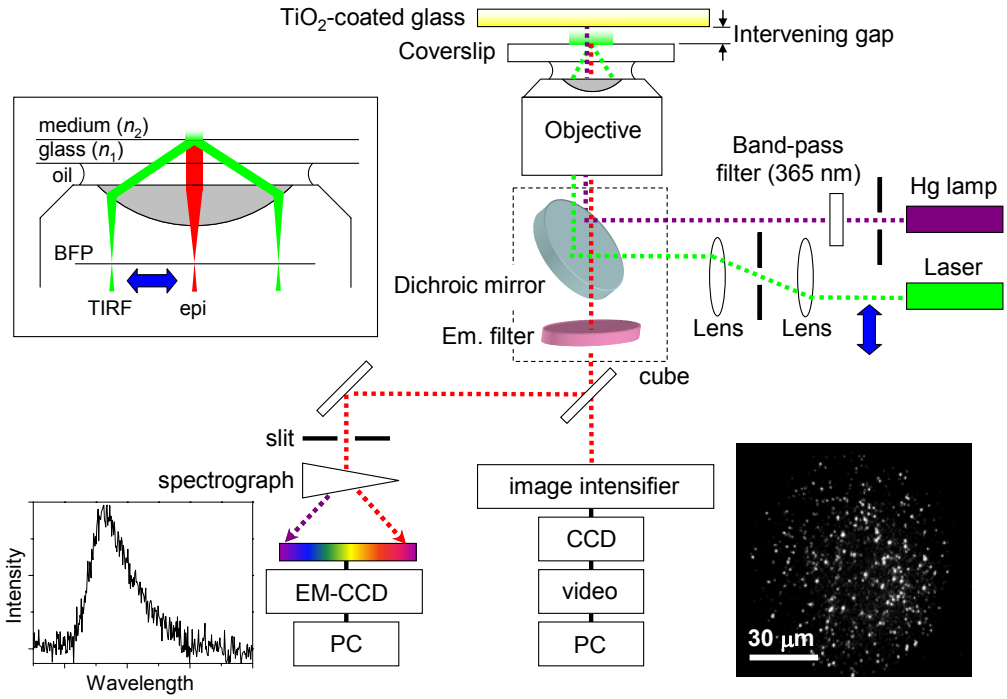

Fig. 1 The optical configuration of objective-type TIRFM based on an inverted microscope.

2.2 Sample preparation

The cover glasses were purchased from Matsunami Glass and cleaned by sonication in a 20% detergent solution (As One, Cleanace) for 6 h, followed by repeated washing with warm running water for 30 min. Finally, the cover glass was washed again with Milli-Q water.

As chemicals for the modification of a dye on the glass surfaces, *N*-[3-trimethoxysilylpropyl]ethylenediamine (TSE) (Aldrich) and Alexa Fluor 532 carboxylic acid, succinimidyl ester (Molecular Probes, see Figure 2) were used without further purification. Cleaned coverslips were immersed in a 1 μM ethanolic solution of TSE for 1 h at room temperature. The silanized glasses were washed with ethanol (Wako) and Milli-Q water, followed by sonication in ethanol and in Milli-Q water to remove any unreacted TSE. The silanized glasses were immersed in a 2 nM acetonitrile solution of Alexa Fluor 532. The reaction was allowed to take place for 1 h and the glasses were then washed several times using ethanol and Milli-Q water, followed by sonication in Milli-Q water. Finally, the glasses were washed with Milli-Q water and dried with an inert gas.

We observed an average of 10-20 single molecules in a 10 × 10 μm^2 area. The number of single molecules observed in this study was much lower than the average density of silanol (Si-OH) groups (4.6 nm^{-2}) on an amorphous silica surface and also much smaller than the possible density of the silanized sites (1.8 nm^{-2}) on a glass surface [28].

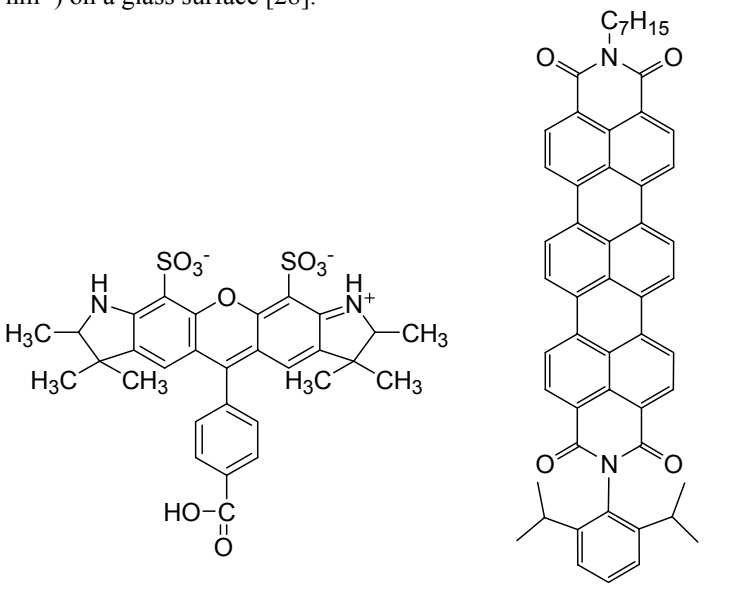

Fig. 2 Molecular structures of Alexa Fluor 532 and terrylenediimide (TDI).

Samples for the single-molecule detection of airborne $^1O_2$ molecules were prepared by first spin-coating a toluene solution of PMMA (40 μl, 10 gl^{-1}) on a clean cover glass at 3000 rpm for 15 s, followed by spin-coating a chloroform solution of terrylenediimide (TDI) (40 μl, 3 nM) at 3000 rpm for 15 s. The sequence of the spin-coating in preparing the samples is very important. The PMMA film should be spin-coated prior to the TDI. In the control experiment, the samples were prepared by spin-coating TDI, followed by spin-coating PMMA. This sample is called the "top-coat". Although PMMA cannot extensively react with $^1O_2$, PMMA can react with the radical oxygen species generated during the TiO_2 photocatalytic reaction, such as HO$^\bullet$ or hydroperoxyl radical ($HO_2^\bullet$). Thus, the underlaying PMMA film allows TDI to selectively react with $^1O_2$ diffusing through the gas phase from the TiO_2 surface, and the contribution of the radicals in the decomposition of TDI is excluded.

A TiO_2 aqueous sol (Ishihara Sangyo, STS-21) was diluted with Milli-Q water (80 vol%), sonicated overnight, and coated on a slide glass (Matsunami Glass) by spin coating at 2000 rpm for 15 s. The resulting TiO_2 film was calcined at 400 °C for 1 h to obtain an optically opaque TiO_2 coated glass plate. The resulting TiO_2 film was irradiated by a UV lamp overnight before the experiment to clean the surface. The film thickness was determined to be 1 μm using a Veeco Instruments Dektak3 surface profiler. The value of the absorbance at 365 nm is about 0.3. The TiO_2 film was irradiated with a 100-W mercury lamp (Ushio, USH-102D) through a 365 nm band-pass filter (Olympus, U-MWU2) (see Figure 1). The gap between the TiO_2 film and the TDI-coated glass was controlled using polyimide films (Nilaco, thickness, 12.5-2000 μm).

3. Single-molecule detection of photocatalytically generated ROS

According to the literatures, it is strongly believed that ROS, such as HO$^\bullet$ and H_2O_2, are generated during the TiO_2 photocatalytic reactions, and diffused into the gas phase [18-20]. To answer whether that

the $HO^{\bullet}$ is sole reactive species or not, we recently proposed a new strategy to detect the airborne ROS diffused from the surface of TiO_2 nanoparticles at the single-molecule level [22].

Figure 3A shows the fluorescence images observed during the 532-nm excitation of single Alexa 532 dyes before and after the UV irradiation of the TiO_2 film with the intervening gap of 12.5 μm in ambient air. The number of single fluorescence dyes (*N*) clearly decreased with the increasing UV irradiation time. It was found that the spatial distribution of ROS reaches about 100 × 100 μm^2 at the surface of the coverslip. In addition, as shown in Figure 3B, the bleaching rates of the dyes significantly decreased with the increasing gap. It should also be noted that the bleaching of dyes was achieved by the very weak UV light. In the absence of a self-assembled monolayer of *N*-[3-trimethoxysilylpropyl]ethylenediamine (TSE) as a linker between the coverslip and the dye molecule, a significant decrease in the bleaching rate of dyes, which are spread over the cover glass using a spin coater, was observed. These results strongly support the fact that the degradation of dyes is caused by the bimolecular reaction with ROS, not by some artifacts such as the UV light scattering.

To identify the origin of ROS, we examined the influence of hole scavengers, such as 2-propanol, on the bleaching process of the dyes. The fluorescence images were obtained after UV irradiation of the TiO_2 film immersed in 2-propanol for 10 min. As shown in Figure 3C, a significant decrease in the bleaching rate was clearly observed when compared with that obtained for bare TiO_2. The most likely explanation is that 2-propanol scavenges photogenerated holes and/or $HO^{\bullet}$ generated at the surface of TiO_2 nanoparticles. Most importantly, it was found that a relatively low bleaching rate of single dye molecules immobilized onto a glass coverslip for the H_2O_2-coated glass was obtained, compared with the TiO_2-coated glass. These results clearly suggest that $HO^{\bullet}$ is not sole reactive species. Considering that gas diffusion coefficients of O_2 and $HO^{\bullet}$ in air are about 0.2 $cm^2\ s^{-1}$, the lifetimes of $HO^{\bullet}$ and $^1O_2$, which are reported to be several tens or hundreds of milliseconds, seem to be sufficient to migrate at least up to the dye-modified coverslip [22].

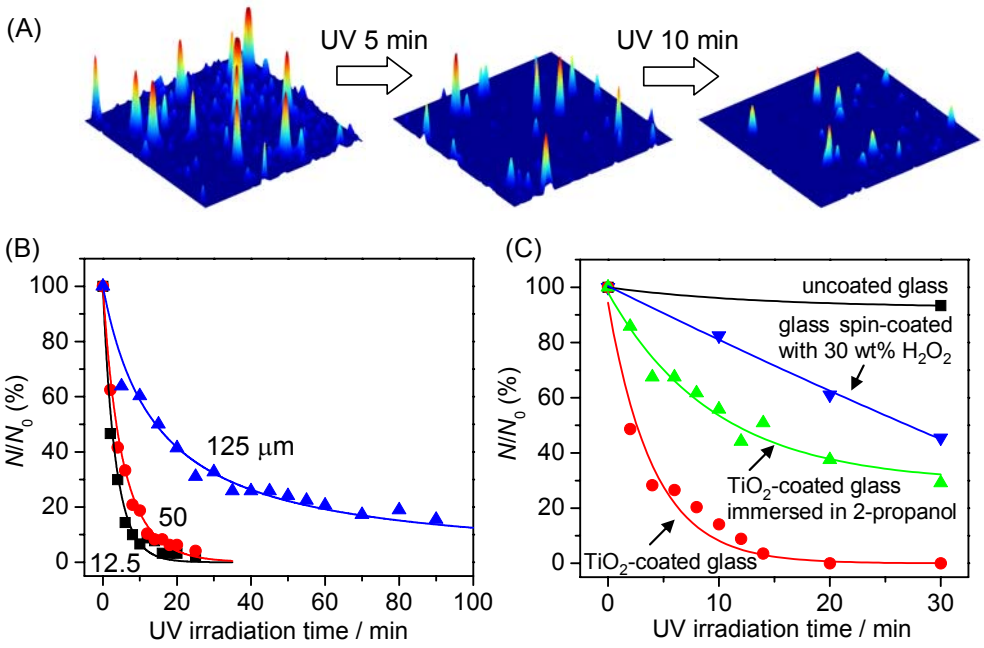

Fig. 3 (A) Fluorescence images observed during the 532-nm excitation of single dye molecules immobilized on the coverslip before and after UV irradiation. (B) Time dependence of the N/N0 values in the gaps of 12.5, 50, and 125 μm. The solid lines are visual guides. (C) Time dependences of the N/N0 values in the 12.5 μm gap observed under various conditions. Copyright 2005 American Chemical Society.

4. Selective detection of $^1O_2$ diffused from the TiO_2 surface

As a next step, we tried to detect an airborne $^1O_2$ molecule diffused from the surface of TiO_2 nanoparticles using TIRFM [23]. The $^1O_2$ molecule is one of important ROS in atmospheric, biological, and therapeutic processes and is also used as a reagent in organic synthesis. Today, it is well-known that $^1O_2$ molecule is a highly energetic oxygen molecule, which can oxidize organic molecules, resulting in the photodegradation. In the early 1930s, Kautsky suggested the possibility that $^1O_2$ molecules might be involved as the reactive intermediate during dye-sensitized photooxygenation reactions [29]. He demonstrated that excitation of sensitizer molecules adsorbed on silica gel caused the oxygenation of acceptor molecules absorbed on a different set of silica gel particles, which are physically separated from the dye-coated ones. From this experimental result, it was concluded that the oxygenation must have involved formation of some metastable species which was capable of migrating in the gas phase from the sensitizer to the acceptor, and suggested that this species was $^1O_2$ molecules.

Recently, it has been reported that $^1O_2$ molecules are directly or indirectly generated via energy or electron transfer reactions between oxygen molecules in the ground state and semiconductor nanomaterials, such as silicon [30], TiO_2 [17], and CdSe quantum dots [31]. Although $^1O_2$ molecules are believed to be generated during the TiO_2 photocatalytic reactions and the formation mechanism has been proposed as a mentioned above, there is no direct evidence to support the diffusion from the surface to the gas phase.

Our strategy to detect $^1O_2$ molecules at the single-molecule level is summarized in Figure 4. Terrylenediimide (TDI) was used as the $^1O_2$ sensor. According to the pioneer work [32], a single TDI molecule should be oxidized by a single $^1O_2$ molecule to form a less fluorescent endoperoxide and successively a strongly fluorescent diepoxide with a spectral blue shift that is easily detected upon 532-nm laser excitation.

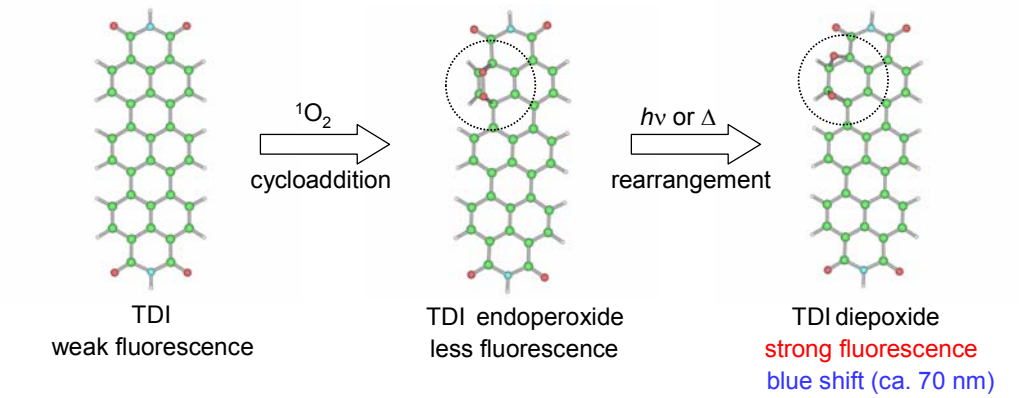

Fig. 4 Single-molecule detection of $^1O_2$ with TDI. Copyright 2006 American Chemical Society.

Figure 5A depicted the single-molecule fluorescence images observed before and after UV irradiation of the TiO_2 film for 5 min. Before UV irradiation, only a few fluorescent spots were observed due to the weak fluorescence of the TDI excited at 532 nm. Due to the lack of sensitivity against the weak fluorescence, almost all TDIs cannot be recognized. Interestingly, after UV irradiation, bright fluorescent spots emerged around the UV-irradiated region as described by the white circles.

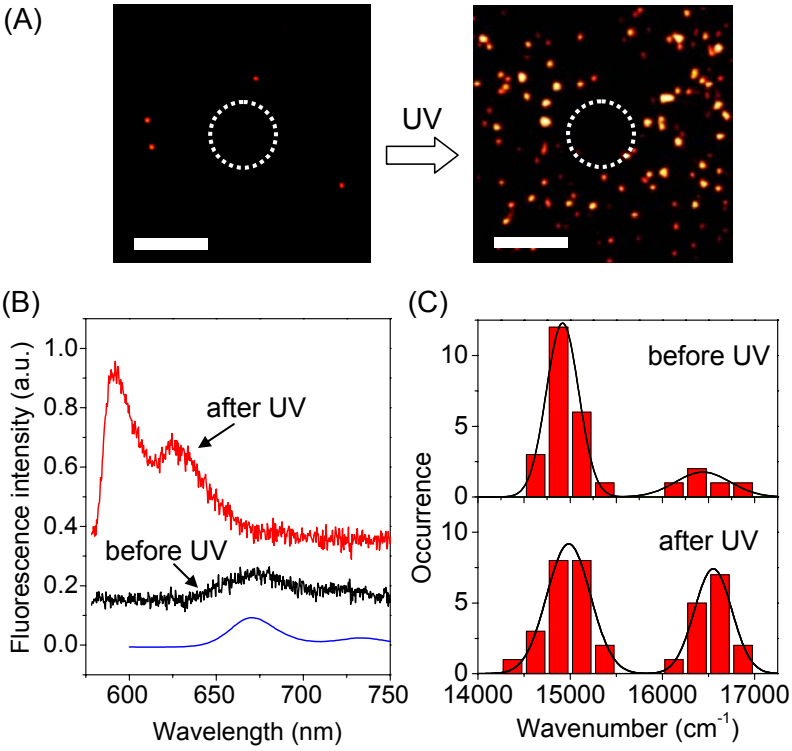

Fig. 5 (A) Fluorescence images of single TDIs spin-coated on the PMMA-coated coverslip before and after UV irradiation for 5 min (scale bars are 10 μm). The intervening gap is 12.5 μm. The bright spots correspond to the blue-shifted, TDI diepoxide. The UV irradiation area is inside the white circle in the images. The absence of dyes at the center of the image after UV irradiation is due to the bleaching of TDI caused by the direct UV irradiation. (B) Typical single-molecule fluorescence spectra of TDI before and after UV irradiation for 5 min. The intervening gap is 12.5 μm. The fluorescence spectra were obtained from excitation at 532 nm and cut below 580 nm by a long-pass filter on the blue edge. The fluorescence spectrum of TDI measured in $CHCl_3$ solution is shown for comparison (blue line). (C) Histogram of the peak wavenumber of the spectra observed before (upper panel) and after (lower panel) UV irradiation for 2 min. Solid lines indicate Gaussian distributions fitted with the histograms. Copyright 2006 American Chemical Society.

To clarify the formation of the TDI diepoxide, the single-molecule fluorescence spectra were measured for each spots before and after the UV irradiation as shown in Figure 5B. Compared to that before UV irradiation, it was found that the spectrum after UV irradiation is blue-shifted by approximately 70 nm and has a strong fluorescence intensity. Thus, the bright fluorescent spots shown in the right image of Figure 5A should be the TDI diepoxide, similar to a terrylene molecule reported by Basché et al [32]. The few bright spots in the left image of Figure 5A also have a blue-shifted spectrum arising from the TDI diepoxide due to the self-sensitization. The fact that the TDI diepoxide shows a strong fluorescence intensity, when compared with that of TDI, is explained as the increase in the absorbed photon due to the blue shift of the absorption spectrum. There speculations were well supported by quantum calculations of optical transitions (Gaussian 03, TDDFT, B3LYP/3-21G*).

Figure 5C shows the histogram of the peak wavenumber of the fluorescence spectra before (upper panel) and after (lower panel) UV irradiation for 2 min. It should be noted that the histogram of the peak wavenumber of the spectra observed during UV irradiation indicates two maxima around 15000 and 16500 cm^{-1}, which are assigned to the parent TDI and TDI diepoxide, respectively. After UV irradiation, the number of TDI diepoxides, that is, the number of $^1O_2$ molecules, clearly increased. It should also be noted that no further spectral blue shift due to multiple attacks of $^1O_2$ was observed in the present

wavelength range. Therefore, the bright spots in the fluorescence images can be regarded as a signal of single $^1O_2$ molecules.

Using this $^1O_2$ nanosensor, the spatial and temporal distributions of single airborne $^1O_2$ molecules diffused from the TiO_2 film have been successfully investigated. Interestingly, several dozen $^1O_2$ molecules are detected even at the intervening gap of 2000 μm as shown in Figure 6. To the best of our knowledge, this is the first example of the single-molecule detection of molecules traveling such a long distance in ambient air. The quantitative analysis enables us to estimate the generation efficiency of airborne $^1O_2$ molecules during the TiO_2 photocatalytic reactions. The $^1O_2$ generation efficiencies during UV irradiation of 5, 10, 15, and 20 min of 11, 9.7, 8.4, and 6.5×10^{-9}, respectively, were calculated from the detected number of $^1O_2$ and the number of photons absorbed by the TiO_2 film.

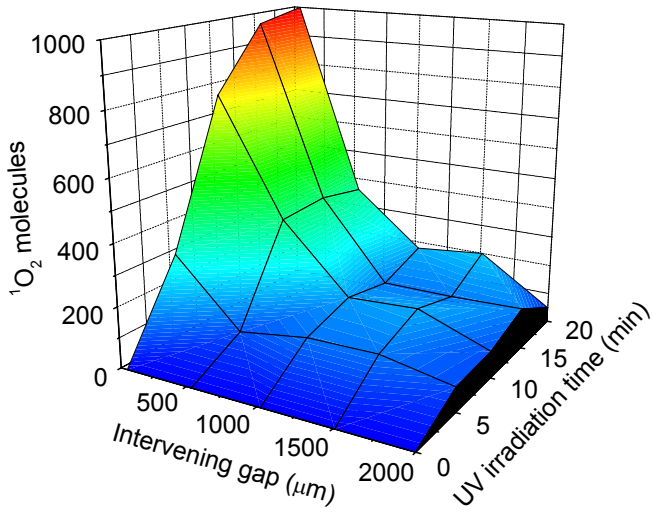

Fig. 6 The spatial and temporal distributions of $^1O_2$ molecules diffused from the surface of TiO_2 film. The observation region is 70×70 μm^2. The intervening gaps are 50, 500, 1000, 1500, and 2000 μm. Copyright 2006 American Chemical Society.

5. Conclusion

We have successfully applied this technique to clarify the bleaching processes of single dye molecules during the remote TiO_2 photocatalytic reactions. Moreover, we detected an airborne $^1O_2$ molecule diffused from the surface of the TiO_2 nanoparticles at the single-molecule level. In the future, the single-molecule spectroscopy will be applicable for various heterogeneous reaction systems as well as photocatalysts. The nanoscale inhomogeneities at the interface or on surface make it rather difficult for ensemble-averaged measurements to analyze the reaction dynamics. The feasibility of studying heterogeneous reactions at the single-molecule level permits us to devise completely new experimental schemes. For instance, one can exploit the possibility to distinguish between the photocatalytically active and inactive molecules (particles). We believe that single-molecule (particle) experiments can provide novel information to understand heterogeneous photocatalytic reactions.

Acknowledgements This work has been partly supported by a Grant-in-Aid for Scientific Research (Project 17105005, Priority Area (417), 21st Century COE Research, and others) from the Ministry of Education, Culture, Sports, Science and Technology (MEXT) of Japanese Government.

References

[1] Ch. Zander, J. Enderlein, R. A. Keller, Eds., Single Molecule Detection in Solution: Methods and Applications, Wiley-VCH, Berlin, 2002.
[2] R. Rigler, M. Orrit, T. Basché, Eds., Single Molecule Spectroscopy: Nobel Conference Lectures, Springer-Verlag, Berlin, 2002.
[3] C. Gell, D. Brockwell, A. Smith, Eds., Handbook of Single Molecule Fluorescence Spectroscopy, Oxford University Press, New York, 2006.
[4] L. Edman, Z. Földes-Papp, S. Wennmalm and R. Rigler, Chem. Phys. **247**, 11 (1999).
[5] L. Zang, R. Liu, M. W. Holman, K. T. Nguyen and D. M. Adams, J. Am. Chem. Soc. **124**, 10640 (2002).
[6] M. B. J. Roeffaers, B. F. Sels, H. Uji-i, F. C. De Schryver, P. A. Jacobs, D. E. De Vos and J. Hofkens, Nature **439**, 572 (2006).
[7] L. Cai1, N. Friedman and X. S. Xie, Nature **440**, 358 (2006).
[8] J. Kirstein, B. Platschek, C. Jung, R. Brown, T. Bein and C. Bräuchle, Nature Mater. **6**, 303 (2007).
[9] C. Jung, C. Hellriegel, B. Platschek, D. Wöhrle, T. Bein, J. Michaelis and C. Bräuchle, J. Am. Chem. Soc. **129**, 5570 (2007).
[10] A. Fujishima, T. N. Rao and D. A. Tryk, J. Photochem. Photobiol. C: Photochem. Rev. **1**, 1 (2000).
[11] M. R. Hoffmann, S. T. Martin, W. Choi and D. W. Bahnemann, Chem. Rev. **95**, 69 (1995).
[12] T. L. Thompson and J. T. Yates, Jr., Chem. Rev. **106**, 4428 (2006).
[13] T. Tachikawa, M. Fujitsuka and T. Majima, J. Phys. Chem. C **111**, 5259 (2007).
[14] K. Ishibashi, Y. Nosaka, K. Hashimoto and A. Fujishima, J. Phys. Chem. B **102**, 2117 (1998).
[15] Y. Nosaka, M. Nakamura and T. Hirakawa, Phys. Chem. Chem. Phys. **4**, 1088 (2002).
[16] Y. Nosaka, T. Daimon, A. Y. Nosaka and Y. Murakami, Phys. Chem. Chem. Phys. **6**, 2917 (2004).
[17] A. Janczyk, E. Krakowska, G. Stochel and W. Macyk, J. Am. Chem. Soc. **128**, 15574 (2006).
[18] Y. Murakami, E. Kenji, A. Y. Nosaka and Y. Nosaka, J. Phys. Chem. B **110**, 16808 (2006).
[19] W. Kubo, T. Tatsuma, A. Fujishima and H. Kobayashi, J. Phys. Chem. B **108**, 3005 (2004).
[20] W. Kubo and T. Tatsuma, J. Am. Chem. Soc. **128**, 16034 (2006).
[21] A. Gomes, E. Fernandes and J. L. F. C. Lima, J. Biochem. .Biophys. Methods **65**, 45 (2005).
[22] K. Naito, T. Tachikawa, M. Fujitsuka and T. Majima, J. Phys. Chem. B **109**, 23138 (2005).
[23] K. Naito, T. Tachikawa, S.-C. Cui, A. Sugimoto, M. Fujitsuka and T. Majima, J. Am. Chem. Soc. **128**, 16430 (2006).
[24] T. Funatsu, Y. Harada, M. Tokunaga, K. Saito and T. Yanagida, Nature **374**, 555 (1995).
[25] D. Axelrod, Traffic **2**, 764 (2001).
[26] F. De Fornel, Evanescent Waves: From Newtonian Optics to Atomic Optics, Springer, Berlin, 2001.
[27] T. Wazawa and M. Ueda, Adv. Biochem. Engin/Biotechnol., **95**, 77 (2005).
[28] H. Kautsky, Trans. Faraday Soc. **35**, 216 (1939).
[29] L. T. Zhuravlav, Langmuir **3**, 316 (1987).
[30] D. Kovalev and M. Fujii, Adv. Mater. **17**, 2531 (2005).
[31] A. C. S. Samia, X. Chen and C. Burda, J. Am. Chem. Soc. **125**, 15736 (2003).
[32] T. Christ, F. Kulzer, P. Bordat and T. Basché, Angew. Chem. Int. Ed. **40**, 4192 (2001).